



# Effect of Cu/(In+Ga) ratios on the secondary phases and the performance of $\text{Cu}_2\text{InGa}(\text{S,Se})_4$ thin film solar cells



Yi-Cheng Lin <sup>a,\*</sup>, Jyun-Ting Huang <sup>a</sup>, Li-Ching Wang <sup>a</sup>, Hung-Ru Hsu <sup>b</sup>

<sup>a</sup> Department of Mechatronics Engineering, National Changhua University of Education, Changhua, Taiwan

<sup>b</sup> Green Energy & Environment Research Laboratories, Industrial Technology Research Institute, Hsinchu, Taiwan

## ARTICLE INFO

### Article history:

Received 1 June 2016

Received in revised form

10 August 2016

Accepted 14 August 2016

Available online 17 August 2016

### Keywords:

Cu(In,Ga)Se<sub>2</sub> solar cell

Secondary phase

Conductive atomic force microscopy

Leakage current

## ABSTRACT

This study investigated the influence of Cu/(In+Ga) ratios on the formation of secondary phases, leakage current, and their effects on the performance in  $\text{Cu}_2\text{InGa}(\text{S,Se})_4$  (CIGSSe) thin film solar cells. An increase in Cu content in the CIGSSe absorber layer was shown to contribute to the growth of grains in that layer as well as the migration of Ga to the surface of the absorber, which increased the energy gap. Excess Cu content resulted in the formation of  $\text{Cu}_{2-x}\text{Se}$  hexagonal nanoplates on the surface of the absorber layer. Conductive atomic force microscopy identified grain boundaries in the CIGSSe absorber layer as the main path involved in the transfer of current through the device. The formation of  $\text{Cu}_{2-x}\text{Se}$  or InSe phases on the surface of the absorber layer expanded the region acting as a current pathway, leading to a breakdown in the P-N junction following the application of negative bias. Measurements of external quantum efficiency under negative bias revealed that secondary phases in the absorber layer act as a recombination center, resulting in a reduction in the  $V_{oc}$  and  $J_{sc}$  of the device. CIGSSe thin film solar cells fabricated by sputtering in this study achieved a maximum conversion efficiency of 13.06%.

© 2016 Elsevier B.V. All rights reserved.

## 1. Introduction

The use of  $\text{Cu}_2\text{InGaSe}_4$  (CIGSe) in solar cells has led to the record-breaking efficiency of 21.7%. This material is also an attractive candidate for thin film photovoltaics, thanks to its high absorption coefficient of  $10^5 \text{ cm}^{-1}$  and band gap that can be tuned to between 1.0 and 1.7 eV simply by controlling the ratios of In/Ga or S/Se [1,2]. Additionally, the  $\text{Cu}_2\text{O}$  films solar cell is also an attractive candidate for thin film photovoltaics [3,4]. During selenization, CIGSe thin films generally form CuSe-based and InSe-based compounds that react with each other to form  $\text{CuInSe}_2$  crystals with a chalcopyrite structure. However, differences in composition, stacking order, and selenization conditions can lead to the formation of secondary phases (such as  $\text{Cu}_2\text{Se}$ ,  $\text{Cu}_{11}\text{In}_9$ , and  $\text{In}_2\text{Se}$ ) on the surface of thin films [5–7]. Most of these secondary phases, which are the result of incomplete reactions, undermine solar cell efficiency [8–10]. The Cu/III ratio also has a profound impact on the characteristics of CIGS films. Formulating an absorber layer with an appropriate Cu/III ratio is an effective method by which to reduce or eliminate the formation of secondary phases, thereby enhancing

the efficiency of the resulting CIGS thin film solar cells. Absorber layers fabricated under Cu-poor conditions (i.e.  $\text{Cu/III} < 0.7$ ) tend to have extremely low conductivity, which results in solar cells with reduced shunt resistance [11]. In contrast, a Cu-rich absorber layer (i.e.  $\text{Cu/III} > 1$ ) produces highly conductive  $\text{Cu}_{2-x}\text{Se}$  secondary phases at grain boundaries at the surface of the absorber layer, which can short-circuit the p-n junction. Even if the  $\text{Cu}_{2-x}\text{Se}$  secondary phases are removed from the surface using KCN etching, the efficiency of the device is still inferior to that of Cu-poor devices [12].

Most previous studies on CIGS absorber layers have focused on absorber crystallinity and its effect on efficiency. Little research has been conducted on the relationship between the appearance of secondary phases in the absorber layer and leakage current in the device. Shin et al. [13] determined that the conduction mechanisms of  $\text{Cu}_{2-x}\text{Se}$  secondary phases produced by Cu and Se defects at CIGS grain boundaries follow the Schottky contact mode, resulting in current leakage. In measuring polycrystalline CdS/CIGS thin films, Azulay et al. [14,15] discovered that grain boundaries narrow the energy band and affect electron transport, which can also lead to current leakage. In the examination of CZTS absorber layers using conductive atomic force microscopy (C-AFM), Li et al. [16] discovered higher current flow at grain boundaries. This effect is an indication that electron mobility in these areas is lower than that in

\* Corresponding author.

E-mail address: [ielinc@cc.ncue.edu.tw](mailto:ielinc@cc.ncue.edu.tw) (Y.-C. Lin).

the surrounding regions, which causes electrons to pass through the areas surrounding the grain boundaries where conductivity is higher. In the analysis of CdS/CIGSse film interfaces, Hegedus et al. [17] discovered that under bias voltage, most photo-generated carriers can be collected with only a minimal loss of electrons. Previous studies have described how grain boundaries in the CIGS absorber layer can affect electron transport resulting in current leakage; however, no previous researchers have analyzed the relationship between leakage current and secondary phases on the surface of the absorber layer or proven that  $\text{Cu}_{2-x}\text{Se}$  secondary phases are the cause of current leakage at the grain boundaries in CIGS. In this study, we used C-AFM to observe the relationship between leakage current and secondary phases in CIGSse thin films. We also sought to obtain clear proof that this relationship exists and determine its influence on solar cell efficiency. Four CIGSse absorber layers with various Cu/III ratios were designed to illustrate the generation of secondary phases, analyze current distribution at grain boundaries on the surface of the absorber layer, and examine the relationship between secondary phases and the location of leakage current. Finally, we investigated the influence of leakage current resulting from CIGS with various Cu/III ratios on solar cell efficiency and external quantum efficiency (EQE).

## 2. Experimental procedure

We began by sputtering In (75 nm) or Cu (75 nm and 150 nm) on soda lime glass ( $20 \times 20 \times 1 \text{ mm}^2$ ) in the area where a Mo back electrode was to be sputtered. We then deposited a  $\text{Cu}_{0.9}\text{In}_7\text{Ga}_3$  ternary target to form a metal precursor with a structure of Cu or In/Cu-In-Ga. This made it possible to engineer precursors with different Cu/(In+Ga) (Cu/III) ratios. The total thickness of the precursor was 800 nm. The structural designs are presented in Fig. 1. We then conducted a two-stage selenization and sulfurization process, in which  $\text{H}_2\text{Se}$  was used for selenization at a holding temperature of 653 K and soaking time of 10 min followed by sulfurization at a holding temperature of 823 K with soaking time of 10 min. A CdS buffer layer was deposited on the completed CIGSse absorber layer using chemical bath deposition, after which transparent conductive i-ZnO and AZO layers were deposited via sputtering. Finally, Al electrodes were deposited by evaporation to complete the glass/Mo/CIGSse/CdS/i-ZnO/AZO/Al solar cell devices with an effective area of approximately  $0.8 \times 0.5 \text{ cm}^2$ . An AM 1.5 solar simulator with light intensity set at  $100 \text{ mW/cm}^2$  was used to measure the efficiency of the resulting solar cells.

Field-emission scanning electron microscopy (FE-SEM, JEOL JSM-6700F) was used to characterize the morphology of the secondary phases and CIGSse films. X-ray diffraction (XRD, JEOL TF-SEM JSM7000F,  $\text{CuK}\alpha$ ,  $\lambda = 1.54052 \text{ \AA}$ ) and Raman analysis (Jobin Yvon T64000 at an excitation wavelength of 532 nm) were used to analyze the secondary phases that formed on the surface of CIGSse films. Grazing incident XRD (GIXRD) revealed a grazing incidence angle of  $0.3^\circ$ – $10^\circ$ . Secondary ion mass spectroscopy (SIMS, IMS-6f)

was used to investigate the depth profiles of the thin film elements. Extraction voltages were set at 10 and 12.5 keV, respectively. The current of the  $\text{O}^{2+}$  ions was set to 80 and 120 nA, which impacted the surface of the samples with energy of 5.5 and 8 kV, respectively. Conductive atomic force microscopy (C-AFM, NT-MDT Solver P47-SP47) was used to investigate the current profiles of secondary phases on the surface of CIGSse film with a bias voltage from +200 mV to –200 mV under a scanning area of  $10 \mu\text{m} \times 10 \mu\text{m}$ . Solar cell EQE (Hitachi QE-3000) was used to investigate the light absorption, and the effect of applying a negative bias to the carrier collection of CIGSse device.

## 3. Results and discussion

### 3.1. Influence of Cu/III ratio on formation of secondary phases

Fig. 2 presents SEM images showing the surfaces and cross-sections of CIGSse thin films of various Cu/III ratios. As shown in Fig. 2(a), when Cu/III = 0.82, the grains in the CIGSse absorber layer are roughly 200 nm in size. An increase in the Cu/III ratio led to an increase in the grain size, indicating that increasing the proportion of Cu promotes grain growth in the CIGSse film. When Cu/III > 1, hexagonal grains became visible in the CIGSse film (Fig. 2(c) and (d)). Based on the composition of the hexagonal grains, as determined using energy-dispersive X-ray spectroscopy (EDX) (Cu/51.6 at.%, In/0.7 at.%, Ga/0%, Se/40 at.%, S/4.7 at.%), these may be  $\text{Cu}_{2-x}\text{Se}$  phases [18,19]. This implies that when Cu/III > 1, the extra Cu led to the formation of  $\text{Cu}_{2-x}\text{Se}$  phases with Se on the surface of the CIGSse film. Table 1 presents the results of EDX and inductively coupled plasma (ICP) analysis of CIGSse films with various Cu/III ratios. These results show that when used to evaluate the same specimen, the EDX results presented higher Cu/III ratios than did the ICP results. The EDX results indicate that the proportion of Cu concentrated in the surface region of the thin film was higher than in other areas. The results in Fig. 2 and Table 1 indicate that when Cu/III > 1, the Cu tended to form  $\text{Cu}_{2-x}\text{Se}$  phases with Se and accumulate on the surface of the CIGSse film.

We used GIXRD with various angles of incidence to characterize the structural differences between the surface and interior of the CIGSse film and to identify  $\text{Cu}_{2-x}\text{Se}$  in the thin film. Fig. 3 presents GIXRD graphs of the CIGSse films with various Cu/III ratios, which were obtained using incidence angles of  $0.3^\circ$ ,  $1^\circ$ , and  $10^\circ$ . The CIGSse films showed diffraction peaks (112), (220/204), and (312/316) at  $2\theta = 27^\circ$ ,  $44^\circ$ , and  $53^\circ$ , respectively [12]. No other secondary phases were observed when the Cu/III ratio was 0.87 and 0.84. At an incidence angle of  $0.3^\circ$ , the specimens with Cu/III = 1.41 and 1.16 displayed (111), (200), (220), and (242) diffraction peaks of  $\text{Cu}_{2-x}\text{Se}$  phase at  $2\theta = 26.6^\circ$ ,  $31^\circ$ ,  $44^\circ$ , and  $51^\circ$  [13], respectively. When the angle of incidence was increased to  $1^\circ$  and  $10^\circ$ , the diffraction peaks of the  $\text{Cu}_{2-x}\text{Se}$  phase weakened considerably. This is a clear indication that most of the  $\text{Cu}_{2-x}\text{Se}$  secondary phases were located at the surface of the CIGSse film. Furthermore, as the Cu/III ratio was

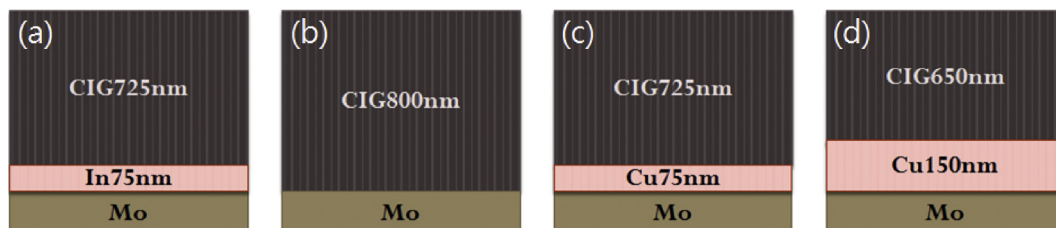


Fig. 1. Schematic illustration of the metal precursors structure of device with various Cu/III ratios: (a) In of 75 nm (Cu/III = 0.84); (b) standard Cu-In-Ga (Cu/III = 0.87); (c) Cu of 75 nm (Cu/III = 1.16); and (d) Cu of 150 nm (Cu/III = 1.41).

Download English Version:

<https://daneshyari.com/en/article/1604905>

Download Persian Version:

<https://daneshyari.com/article/1604905>

[Daneshyari.com](https://daneshyari.com)